

Article

Simulation of Spatiotemporal Land Use Changes for Integrated Model of Socioeconomic and Ecological Processes in China

Honglei Jiang ^{1,2} , Xia Xu ^{1,2,*}, Mengxi Guan ^{1,2}, Lingfei Wang ^{1,2}, Yongmei Huang ^{1,2} and Yinghui Liu ^{1,2}

¹ State Key Laboratory of Earth Surface Processes and Resource Ecology, Beijing Normal University, Beijing 100875, China

² Faculty of Geographical Science, Beijing Normal University, Beijing 100875, China

* Correspondence: xuxia@bnu.edu.cn

Received: 19 May 2019; Accepted: 27 June 2019; Published: 2 July 2019



Abstract: Land use/land cover changes (LULCC) have been affected by ecological processes as well as socioeconomic and human activities, resulting in several environmental problems. The study of the human–environment system combined with land use/land cover dynamics has received considerable attention in recent decades. We aimed to provide an integrated model that couples land use, socioeconomic influences, and ecosystem processes to explore the future dynamics of land use under two scenarios in China. Under Scenario A, the yield of grain continues to increase, and under Scenario B, the yield of grain remains constant. This study created a LULCC model by integrating a simple global socioeconomic model, a Terrestrial ecosystem simulator (TESim), and a land use allocation model. The results were analyzed by comparing spatiotemporal differences under predicted land use conditions in the two alternative scenarios. The simulation results showed patterns that varied between the two scenarios. In Scenario A, grassland will expand in the future and a large reduction in cropland will be observed. In Scenario B, the augmented expansion of cropland and a drastic shrinkage of forest area will be the main land use conversion features. Scenario A is more promising because more land is preserved for ecological restoration and urbanization, which is in line with China’s Grain for Green Program. Economic development should be based on ecological protection. The results are expected to add insight to sustainable land use development and regional natural resource management in China.

Keywords: sustainability; socioeconomic influence; ecosystem processes; land use change model; scenario simulation

1. Introduction

Research on LULCC has attracted the attention of many scholars due to its important role in global climate change, food security, soil degradation, and biodiversity [1–4]. We often use different simulation methods to study LULCC across landscape [5,6], region [7–10], and global scales [11]. The spatially explicit model of land use change is an excellent tool for quantitatively describing the process of land use change and extending our understanding of the process [12,13]. The purpose of land use change simulation is to predict the spatial pattern of change. Therefore, two problems are posed that need to be solved: How will the amount of land use change? Where will land use change occur? These two problems are considered “number” and “position” problems [14].

LULCC models are powerful tools for analyzing driving forces and processes, understanding causes and consequences, and projecting possible future land use patterns [15,16]. Depending on the research objective, the relevant LULC models can be divided into two categories: (i) empirical-statistical

models; and (ii) spatially explicit models. The first is fitted using mathematical equations and carry out statistical analyses such as the regression of factors that affect LULCC, such as System Dynamics (SD) models [17]; however, few of them include social factors and policy implications, only providing the quantity demand [18]. The second is widely adopted to simulate LULCC explicitly, such as the cellular automata (CA) model [19], the Future Land Use Simulation (FLUS) model [20], and Multi-Agent system (MAS) models [21]. In particular, the Conversion of Land Use and its Effects (CLUE) model is an excellent tool for interpreting land use change processes [22,23]. It has been successfully applied to modeling land use change explicitly at different scales [24–26]. These spatial allocation models are primarily used to determine the pattern and process of LULCC and then project the locations of future changes; however, it is still difficult to simulate the effect of socioeconomic influences on LULCC, because of a large number of interacting factors that need to be taken into account, such as environmental changes, scientific and technological progress, policy changes [27]. Furthermore, dynamic ecological processes are rarely involved in these models, and most currently published studies have used a static soil property database as an indicator of ecological effects to simulate simplified landscapes [28,29].

Land systems are dynamic and are influenced by the interactions between humans and the environment [30–32]. Therefore, the drivers of LULCC basically originate from two aspects: (i) natural power; and (ii) socioeconomic drivers. The first aspect, natural power, includes climate change and ecosystem processes. Some key processes (e.g., net primary productivity) enable various lands to sustain Earth's life support systems, which, in turn, provide ecosystem services [33,34]. The second aspect, socioeconomic drivers, include economic growth and demographic increase [35,36]. The increase in population and economy has placed unprecedented pressure on cultivated land. The UN projects that the global population will increase from 7.3 billion in 2015 to 9.7 billion in 2050, with an increasing demand for resource-intensive meat and dairy products [37–39]. This increase has led to a higher demand for arable lands around the world [40,41]. This is especially true in China. Since the onset of reform and openness that started in 1978, China's population has grown by nearly 1.4 times [42]. Rural land reforms in China have been improving domestic agricultural production in order to satisfy the nation's food demands. However, with such a large population, over 10% of agricultural products still need to be imported in order to meet current food demands [43–45].

Feeding a rapidly increasing population triggers the conversion of many landscapes from natural vegetation cover to agricultural land use unless an increase in crop yield can reduce the need for new cropland [46–49]. Although an increase in yield can contribute to improved production, the world's arable land may undergo even further expansion by 2050 [50,51]. Even so, improved yield has been credited with the prevention of transforming uncultivated land to arable land [52]. In recent decades, the yield growth rate for most crops has been decelerating, and China has experienced this phenomenon with pronounced fluctuations [53,54]. Yield change is one of the key factors exerting influence on cropland demand. However, few studies have focused on the effect of yield change on LULCC. Exploring land use change, especially when cropland is involved, with the driver of changes in yield is essential for coordinating human–land relationships and achieving regional sustainable development.

In the holistic human–environment system, three pillars of sustainability—society, economy, and ecology—are emphasized [55]. However, knowledge gaps still exist in simulating future land use pattern, integrating socioeconomic and dynamic ecological condition to LULCC model. In our work, land use patterns have been projected by using some drivers, including yield change and key ecosystem processes, which are discussed in our paper. Several interesting questions are included in this study: (1) How can we construct an integrated model that combines socioeconomic and ecological processes and land use? (2) What are the quantitative features and spatial patterns of land use types in the future? (3) In the context of crop yield change, what guides can we provide to facilitate the sustainable use of natural resources? The results are analyzed by comparing different projected land use spatial patterns and quantitative structures under two yield-changing scenarios.

2. Materials and Methods

In this work, we propose an integrated model to project land use patterns in China that result from the influences of grain yield and ecosystem processes. The proposed model consists of three linked components: the first is a simple global socioeconomic model that provides a quantity requirement for each land sector; the second is a terrestrial ecosystem simulator that identifies the land use suitability of a site; the third is a spatial modeling component using a land allocation model. Different food consumption levels result in various demands for land use sectors. Different ecosystem processes also affect land use suitability, for instance, the loss of nutrients caused by soil erosion processes in cropland weakens its sustainable utilization. Therefore, site ecological conditions, as well as socioeconomic factors, are considered the primary drivers of spatial patterns in land. By linking socioeconomic and ecological processes, from quantity to spatial pattern, we created the integrated model.

2.1. The Global Socioeconomic Model

The global socioeconomic model quantifies the demand for areas of different land use types by simulating the consumption and production of agricultural commodities. At the same time, global consumption and production maintain a balance through international trade flows among countries at the global scale. The global socioeconomic model was developed from the Global Food System model (GLOBFOOD) [56]; it is composed of 160 country units and has four submodels: consumption, production, land use, and trade (Figure 1). The detailed description of GLOBFOOD can be found in Jiang et al. [56]. Here, we highlight some principles established in the model.

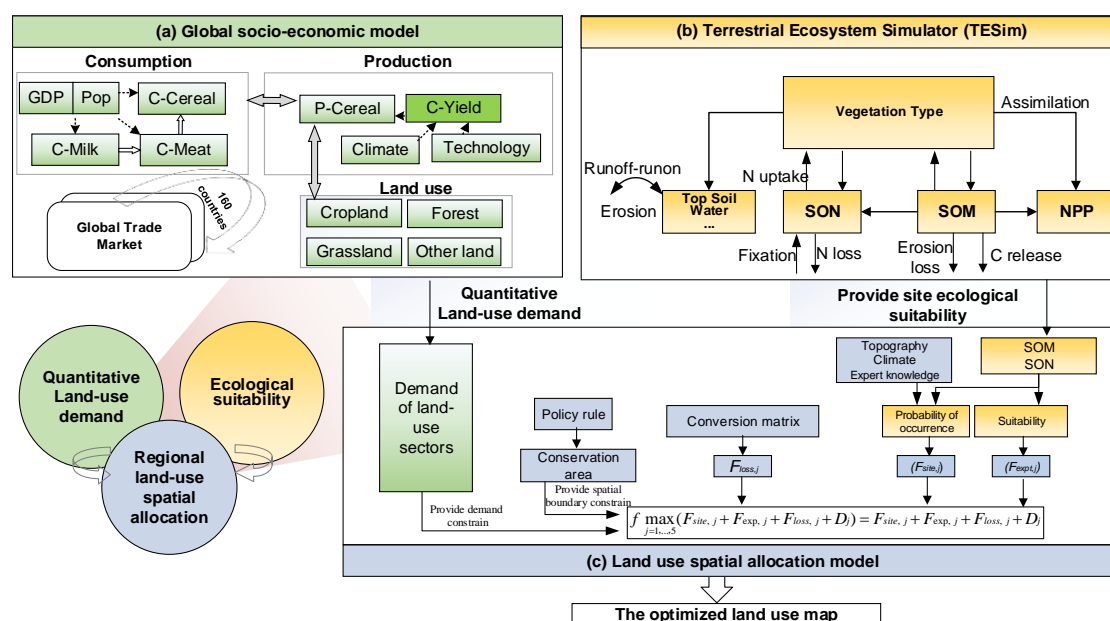


Figure 1. The framework of the linked model. The model integrates three modules: (a) a global socioeconomic model [56], (b) a land use allocation model [8,9], (c) a Terrestrial Ecosystem Simulator [10]. GDP = Gross Domestic Product, Pop = population; C-Cereal = consumption of cereal, C-Milk = consumption of milk, C-Meat = consumption of meat; P-Cereal = production of cereal, C-Yield = crop yield; N uptake = nitrogen uptake, N loss = nitrogen loss, C release = carbon release, SOM = soil organic carbon, SON = soil organic nitrogen.

In the consumption module (Figure 1a), a growing population creates a persistent demand for food consumption. The pressures on food consumption come not only from the growing population but also from the food consumption per capita and food preferences. The consumption demand is calculated from the consumption per capita, which is influenced by the population growth and the

GDP per capita in each country. The three major types of global food consumption structures are cereal, meat, and milk consumption. The relationship for meat consumption per capita can be described as

$$C_t = C_0 * (G_t/G_0)^k \quad (1)$$

where C_t and C_0 represent the meat consumption per capita at time t and a reference baseline, respectively; G_t and G_0 represent the GDP per capita at time t and a reference baseline, respectively; k is a parameter that is calculated by applying a regression relationship between a country's historic consumption per capita and its GDP per capita changes. Cereal and milk consumption can be described with a similar formula.

In the production module, the per capita consumption in each region is converted into the regional demand for different land use sections by including the interregional trade of crops and animal products. The production of crops is influenced not only by natural conditions, such as climate change, but also by technological advances, such as yield increase.

In the land use module, the major conversions between cropland and other land sectors are determined by different food demands. The Land Required for Food (LRF) is adopted here to represent the requirements for cropland [57]. The LRF (unit: ha) can be calculated using this equation:

$$LRF = P * F/Y \quad (2)$$

where P represents the size of the population (capita), F represents food supply (kg/capita/year), and Y represents the yield of cropland (kg/year/ha).

As part of the world economy, China plays an active role in global food trade and is influenced by others as well. In the global trade market module, agricultural commodities are balanced between production and consumption through import and export among countries.

2.2. Terrestrial Ecosystem Simulator (TESim)

A regional ecosystem model (TESim, Figure 1b) was used to simulate ecosystem production, nutrient cycling for terrestrial ecosystems, regional carbon balance, and local soil erosion. The parametrization, validation, and application of the TESim formulation, without land use change, were specifically described in earlier publications [8,9,11]. The two output variables used in the present study are (i) SOM (Soil organic matter) and (ii) SON (Soil organic nitrogen). The two variables, derived from the dynamic ecological model rather than an existing static database (e.g., Harmonized World Soil Database), were deliberately chosen to especially show the local ecological effects of land use patterns and evaluate site suitability.

2.3. Land Use Allocation Model

The principles of the Conversion of Land Use and its Effects (CLUE) model [22] were adopted in our study (Figure 1c). The CLUE model applies many constraints and transformation rules, including site suitability factors and land use stability factors. Through iterative calculations, land-use types are gradually assigned to a certain utilization, reflecting accurate simulation results that are spatially explicit [11–14]. Based on the classification of LULC from Chinese Academy of Sciences (<http://www.resdc.cn/>), five types of land use categories were used: cropland (CROP), grasslands (GRAS), forests (FORE), built-up land (BUIL), and others (OTHE) were used as the five types of land-use categories in China. Land use spatial patterns, overall, are dominated by ecosystem processes. Thus, we coupled ecosystem processes with land use change processes. Xu et al. [9] reported their evaluation of the TESim model integrated with a land use allocation model, and the parameters can also be found in their studies [8,9].

Equation (3) was used to allocate a specific land use type to each cell to achieve the maximum overall suitability:

$$LU(r) = LT_j, \quad \text{if } \max_{j=1,\dots,5} (F_{site,j} + F_{exp,j} + F_{loss,j} + D_j) = F_{site,j} + F_{exp,j} + F_{loss,j} + D_j \quad (3)$$

where $LU(r)$ is the land use variable, r is the spatial location variable (r^{th} grid cell), and LT_j is the value of $LU(r)$ that specifies the type of land use. In the present study, $LT_j = \text{CROP, GRAS, FORE, BUIL, or OTHE}$ for $j = 1, 2, 3, 4, \text{ and } 5$, respectively. $F_{site,j}$ is a site probability factor that is statistically derived from the relationship between the land use type and site variables, such as SOM, SON, topography (i.e., elevation and slope), and population. $F_{exp,j}$ is the suitability factor—a weighted average of the fuzzy expert membership functions. $F_{loss,j}$ is an index derived from land use change data to quantify the probability that one land use type is transferred to another between 2000 and 2005; therefore, $F_{loss,j}$ is inversely proportional to land use stability. D_j is a series of constants estimated by socioeconomic demands for a specified land use structure. Then, land units (grid cells) are allocated to types that have the maximum suitability and stability, adjusted by the demand.

Logistic regression was used to calculate the probability of the occurrence of events; the argument is used as a predictive value that may explain the relationship between site variables and land use types appearing at this site. The advantage is that variables can be either continuous or categorical. $F_{site,j}$ was computed with a multivariate logistic regression, as follows:

$$F_{site,j} = \frac{\exp(a_j + \sum_{\xi=1}^m b_{j\xi} X_{\xi})}{1 + \exp(a_j + \sum_{\xi=1}^m b_{j\xi} X_{\xi})} \quad (4)$$

where $j = 1, \dots, 5$ denotes the different land use types. X_{ξ} for $\xi = 1, \dots, 9$ is a series of site variables, including socioeconomic and ecological variables in our case, namely, (1) population density, (2) elevation, (3) slope, (4) mean annual temperature, (5) mean annual precipitation, (6) cumulative daily mean temperature during the growing season, (7) precipitation during the growing season, (8) SOM, and (9) SON. After TESim outputted the parameters of SOM and SON, the two variables were then inputted to the land use spatial allocation model, and the other seven variables were derived from meteorological or topographical data. The coefficients a_j and $b_{j\xi}$ were fitted by regressing a land use variable on all of these site variables. The land use variable equals 1 if the site is currently occupied by land use type j , and it is zero otherwise.

$F_{exp,j}$ was calculated using Equations (5) and (6):

$$F_{exp,j} = \sum_{i=1}^n w_i f_i(x_i) \quad (5)$$

$$f(x_i) = \begin{cases} [1 + (\frac{x_i - x_{i0}}{B_i})^2]^{-1} & , x_i < x_{i0} \\ 1, & \text{otherwise} \end{cases} \quad (6)$$

where W_i is the weight and is determined by the relative correlation between land use and the i^{th} influence factor x_i , and $f_i(x_i)$ is the fuzzy membership function that was constructed to estimate site suitability. X_{i0} and B_i are parameters set up according to empirical expert knowledge and Food and Agriculture Organization (FAO) land classification.

$F_{loss,j}$ was used to calculate the loss likelihood in Equation (7):

$$F_{loss,j} = \sum_{i=1, i \neq j}^q \mu_{ij} \quad (7)$$

where $q = 6$ in this work, indicating the total number of land use types. Equation (7) requires at least two maps of land use at different time periods to identify the loss likelihood which land use type i is transferred to land use type j . The variable μ_{ij} is equal to the approximate number of sites transferred to land use type j in the second (later) map divided by the total number of sites of land use type i in the first (earlier) map.

2.4. Coupling the Land Use Allocation Module with the Terrestrial Ecosystem Simulator and Global Socioeconomic Module

We linked the land use change processes with the global socioeconomic processes and ecosystem processes in China via an interactive procedure. The framework for combining the three models to form the integrated model is shown in Figure 1, and some of our steps are as follows: (1) Different demands for land use quantity, the output of the global food model, are input into land use allocation model as a quantity constraint for each land use type; (2) TESim was run to generate an initial land use map and identify the ecological effects, and the outputs for SOM and SON were then inputted to the land-use allocation model as factors that evaluate land use suitability; (3) the land-use allocation model was applied to allocate areas of various land-use types to each spatial grid with the best suitability; Steps 1–3 form the first round of simulations. The given land-use area is expected to be achieved when all spatial grids are allocated to a specific land use type; (4) as the newly adjusted variables may not meet the set demand, we implemented several rounds by modifying the interactive constant D_j (in Equation (3)) in the land use allocation model. The initial condition of the interactive constant was 0. If the area of the initial distribution was greater than demand, we reduced the iteration variable and vice versa. Then, we gradually modified the interactive constant until it met the imposed aggregate quantity. This signaled the convergence of the procedure and the iteration stopped; (5) if the program is divergent and there is no rational land use pattern with the largest suitable area, then we edit the land use demand in the global socioeconomic model.

2.5. Data Preparation

Our research required data obtained from various official sources. The data used included three land use maps of China with a resolution of 1 km that quantify land use changes for 2000, 2005, and 2010 from the Chinese Academy of Resources and Environment Science Data Center (<http://www.resdc.cn/>). $F_{loss,j}$ (in Equation (7)) was derived from the Markov matrix calculated from two land use maps for 2000 and 2005, and the land use map for 2010 was used to validate the model. A regional DEM with a 50 m resolution from the State Bureau of Surveying and Mapping (<http://en.sbsm.gov.cn/>) was used to calculate topographical variables such as elevation and slope. Spatial variables were resampled using ArcGIS at a linear resolution of 10 km. All of the spatial variables above were resampled using ArcGIS (Version 10.2, America, <https://www.esri.com/>) at a linear resolution of 10 km. Meteorological data for 685 weather stations were downloaded from China National Weather Service (<http://www.cma.gov.cn/>) for the time period from 2000 to 2007, and the data were interpolated into raster maps with a resolution of 10 km and then used to drive TESim. Meteorological data and topographical variables were also used to identify $F_{site,j}$ (in Equation (4)) and W_i in $F_{exp,j}$ (in Equation (5)). Socioeconomic data, such as population, GDP per country, and consumption and production of crop, were collected from the National statistics department (<http://www.stats.gov.cn/tjsj/nds/>), and FAO (<http://www.fao.org>) was used to drive the global socioeconomic model and generate different scenarios.

2.6. Scenario Development

Scenarios of land use change help to explore possible trends under a set of simple conditions. In the current context of rapid economic development and climate change, the scenario approach is one of the most efficient tools in many sciences and is characterized by different considerations of a storyline.

Based on the background of China's yield, two plant-yield scenarios for China were selected. Scenario A: The yield continues to rise in accordance with the existing rate, leading to lower arable requirements; however, recent productivity growth has slowed down as the profits from the new technology and advanced farming practices in some sectors become outdated. Moreover, excessive use of chemical fertilizers degrades the quality of soils and shrinks groundwater supplies [54]. So Scenario B was developed: After reaching the current level, the yield stays constant, but because of increasing consumption, the cropland requirements will rise (Figure 2b). The parameters for the global socioeconomic model are shown in Table 1, and the peak consumption is described in the following paragraphs.

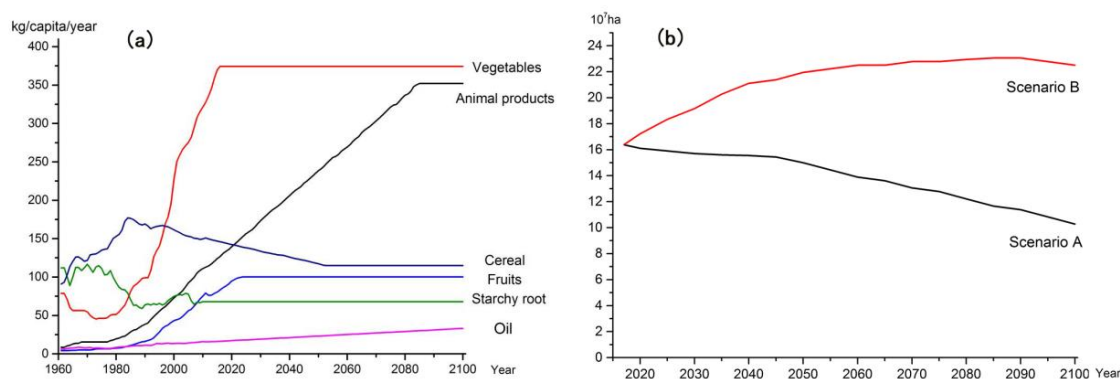


Figure 2. Projections of consumption per capita until 2100 (a), and Arable Land Required for Food (LRF) for China in two scenarios (b).

Table 1. The parameters for the global socioeconomic model.

Variables	Parameters	Description
Population	* [−1%, 1%]	
GDP	* [−4%, 4%]	At country level from Xu et al. [9]
Cereal consumption	* [−2%, 2%]	
Meat consumption	0.5 [−10%, 10%]	Extension of the regression relationship between a country's historic consumption per capita and its GDP per capita changes
Milk consumption	0.3 [−10%, 10%]	
Land degradation or natural loss	−0.033 [−10%, 10%]	Soil is degraded mainly through deforestation and agricultural activities. We assigned 0.2% of the cropland and 0.5% of the natural forest as degraded into grassland and a grassland degradation rate of 0.3% (FAO, 2003; Jiang et al. [56])
Trade (integrated market level)	0.4 [−50%, 50%]	This determines the rate of trade to meet demand
Yield changes due to technology advancement	Scenario A: 0.02 [−10%, 10%] Scenario B: 0	The yield in Scenario A will keep increasing; The yield in Scenario B will keep increasing at the same rate as in Scenario A until the yield reaches the current level.

Notes: The parameters were set with a mean value and an uncertainty level, e.g., 0.5 [−10%, 10%] is equal to [0.4, 0.6], and the uncertainty level was estimated by the standard deviation between countries. The * symbol means real data at the country level that can be used by the model directly, and other factors are considered as relative changes compared with year 2005.

We identified all of the changes in the future per capita consumption by comparing developed countries or regions, such as the United States of America (USA) and the European Union (EU), and

the predictions were divided into two categories: plants and animals. On the basis of the number of plants, we selected five aspects: cereal, oil crop and vegetable oil, starchy roots, fruits, and vegetables. With regard to animals, we calculated the sum of animal production/consumption, including animal fats, eggs, meat, milk, and offal.

When predicting the consumption peak in China, we referred to the US and the EU consumption structure, which has reached maturity (Figure 2a) [57]. Annual per capita cereal consumption in the EU and the US is 120 kg and 110 kg, respectively. We chose the average of both as part of our case. When cereal consumption reaches 115 kg per capita/per annum, it remains stable. According to the current rate of growth, oil consumption will not reach the level consumed by the USA and the EU even by the year 2100; thus, we followed the current growth rate and did not set consumption peaks. Regarding annual per capita fruit consumption, both the EU and the US remain at approximately 100 kg. Therefore, we set China's peak to occur when fruit consumption reaches 100 kg and will remain stable thereafter. The consumption of starchy roots has fluctuated since the 1990s; therefore, we set the average of these years, 67.64 kg, as the future consumption rate. Regarding vegetable consumption, China's vegetable supply is ranked first in the world and thus cannot be set using other countries' consumption peaks. Therefore, we referred to the data from China's National Bureau of Statistics. While vegetable consumption in both urban and rural areas is declining now, we assume that future vegetable consumption corresponds with rates that are expected to increase until reaching the 2015 levels, after which they will stay constant. For animal products, we used the sum of the five animals' production/consumption, and referred to the EU's consumption, which stabilized once it reached 350 kg per capita/per annum.

3. Results

3.1. Model Validation

The global socioeconomic model was applied to simulate land use requirements for the year 2010 in different sectors. Here, we compared the simulation results with the monitored area (Figure 3). The results indicate that in the simulated demand, the cropland and built-up areas are relatively similar to the corresponding classes in the actual land use demand for 2010, but the area of forest and grassland was overestimated by 8.2% and 5.8%, respectively. This overestimation bias might be related to the decrease in the food stock in recent decades. Specifically, consumption of grain has outpaced the production for years. Food stocks were used to make up for the deficit in production, alleviating the demand for land. However, we did not include food stock as they were too random to be simulated either on the country or international level. So the land use was overestimated to some extent [58]. The spatial verification of the model was performed in Xu et al. [9]. We regard the driving forces, such as terrain, elevation, and meteorological factors, to be unchanged, so the model was adopted in the next analysis.

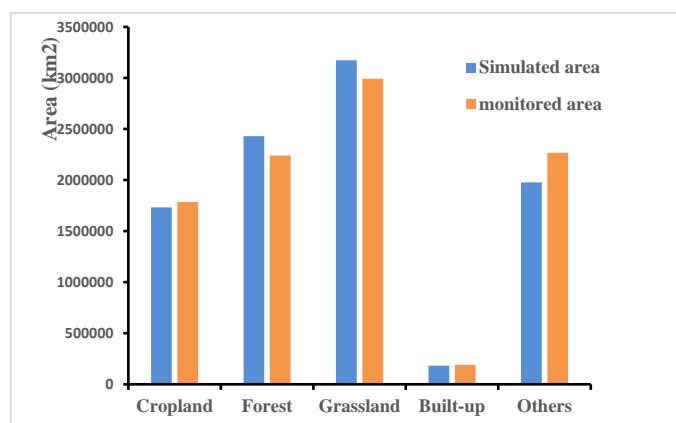


Figure 3. Comparison between simulated and monitored land use areas.

3.2. Conversion Matrix of Land Use Types

The conversion rate of different land use types was calculated by using quantitative transition features of different land use types between 2000 and 2005 using a Markov chain model (Equation (7)). Table 2 shows the quantification of the statistical frequency values of land use change and the transition relationship values of each land use type. The smaller the transition indices, the smaller the change in land use type and vice versa. The two largest transition indices were built-up and forest areas, with 52.66% and 41.36%, respectively. The increase in forest was mainly due to the strengthening of environmental awareness. The expansion of built-up was attributed to the rapid economic development and urbanization, which also took responsibility for higher transition indices in unused land with the proportion of 38.82%. The conversion rates of grassland and water areas were smaller than those of others, with values of 23.46% and 22.28%, respectively.

Table 2. Land use conversion rate comparison for two years (2000, 2005) (%).

	Cropland	Forest	Grassland	Water Areas	Built-up	Other
Conversion rate	34.96	41.36	23.46	22.28	52.66	38.82

For significant ecologically protected lands, such as water areas, considering the practical situation, the conversion rule was set to 0, which means that significant ecologically protected lands are not allowed to be transferred to any other land use type during the space allocation process.

The land use change matrix (Figure 4) shows the situation of various land use type transformations. The more intensive transitions between different types of land use are reflected in the mutual conversions among cropland, forest, and grassland, where 12.29% of cropland had been converted into grassland and forest. The probability of grasslands being converted into cropland and forest was 6.76% and 7.24%, respectively. A significant change was also reflected in the expansion of built-up areas, with 26.90% of cropland, 5.2% of forest, and 3.02% of grassland being converted into built-up areas. This may lead to the degradation of the ecological environment, thereby affecting the existing urban patterns, economic development, and the process of urbanization.

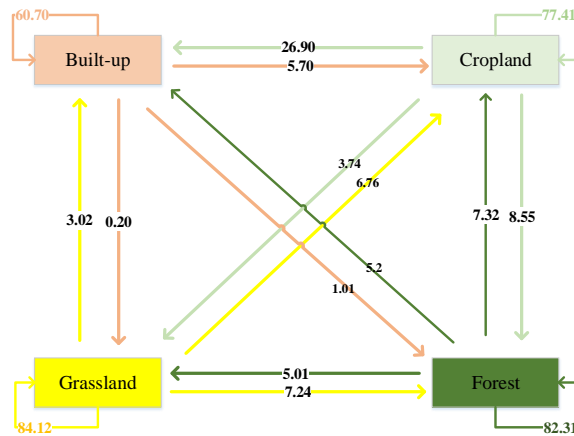


Figure 4. Transition probabilities between 2000 and 2005 (%).

3.3. Quantifying Change in Projected Land Use

Figure 5 shows the proportional composition of each land use type in different scenarios simulated by the integrated model. In Scenario A, cropland yield is expected to increase at the current rate. The expected trend of cropland area change is expected to gradually decline as forest, grassland, and built-up areas increase. The projected cropland in 2080 is expected to be 27.37% lower than that in 2020. Forests, grassland, and built-up areas will increase by 6.66%, 4.50%, and 88.18%, respectively. In Scenario B, cropland yield remains constant and the proportion of cropland area is projected to show a significant increase, reaching approximately 29.41% between 2020 and 2080. Forest, grassland, and built-up areas are expected to decrease by 11.15%, 5.88%, and 29.03%, respectively. In addition, when we compared land use in 2020, 2050, and 2080, excluding cropland, the different land use types in Scenario B all presented significantly smaller areas than those in Scenario A.

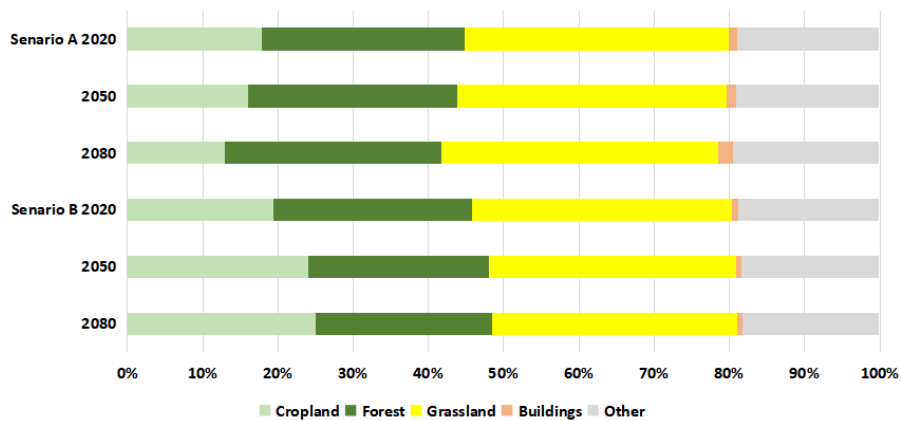


Figure 5. The proportion of land use types in two scenarios (%).

3.4. The Spatial Pattern of Land Use

Figure 6 presents the land use spatial distribution pattern with significant spatial heterogeneity in China. Overall, the pattern had not changed very much since the distribution patterns of various land use types is formed by a long historical development process. Agricultural crops have high solar and water requirements. Cultivated land is mostly near the eastern coastal and central areas, the Northeast China Plain, the North China Plain, and the Yangtze River Valley. They have predominantly humid climates, flat terrain, superior natural ecological conditions, and highly concentrated populations. China’s forests are mainly distributed in the north along a sand prevention belt, along the desertification control areas, and in the south and northeast mountain hilly areas. These areas have a relatively

good ecological environment and small populations, so they experience less human disturbance. Grasslands are mostly in the northwest. They are predominately the arid and semi-arid regions of the Inner Mongolian Plateau and Qinghai–Tibet Plateau ecological barrier area, which comprise the largest cold-desert steppe and natural grasslands in China. Built-up areas are primarily in the densely populated eastern coastal regions, basins, and plains and intersect with cropland areas.

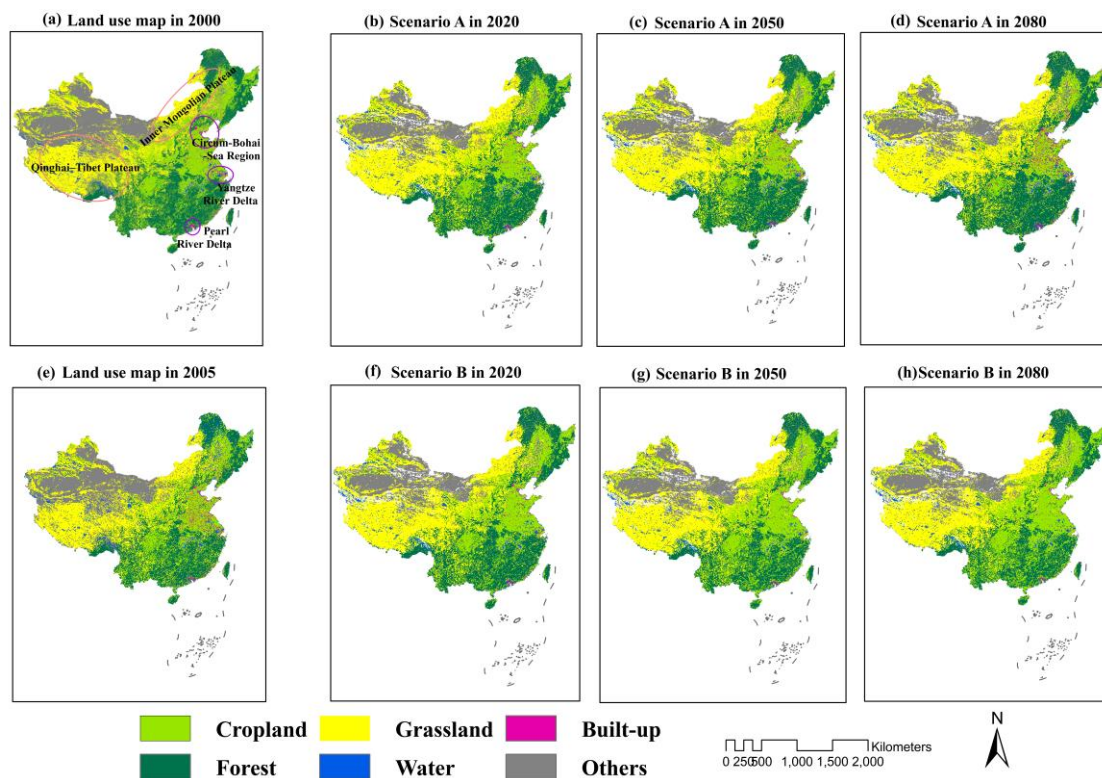


Figure 6. Different land use patterns in 2000 and 2005. Two projected scenarios for 2020, 2050, and 2080.

Figure 7 shows some hotspots of LULCC in the two scenarios. Generally, the distribution changes in large-scale land cover are less pronounced in the short term owing to the long development of the formation of a land use type. In Scenario A in 2080, in Northern China, the Loess Plateau (Figure 7a) and Inner Mongolia farming-pastoral areas will see some croplands being converted into grassland or forests. The land use change will most likely be reforestation and afforestation of cropland. Built-up land is expected to expand extensively, mainly at the expense of high-quality cropland; this will most likely be mainly observed in the eastern coastal regions of China such as the Circum-Bohai-Sea Region (Figure 7b), the Yangtze River Delta, and the Pearl River Delta. The initial growth in urbanization is expected to occur in the North China Plain and in the southeast coastal areas in 2020. This may lead to the conversion of paddy to artificial infrastructures. However, in Scenario B, the cropland areas are expected to show a long-term increase. In the Sichuan Basin, the northwest agro-pastoral transitional zone, the East Inner Mongolia region, the south inter-mountain basin, and the edge of the oasis at the foot of the Tianshan Mountains, grassland or forests are expected to be converted into arable lands, triggering deforestation (Figure 7c).

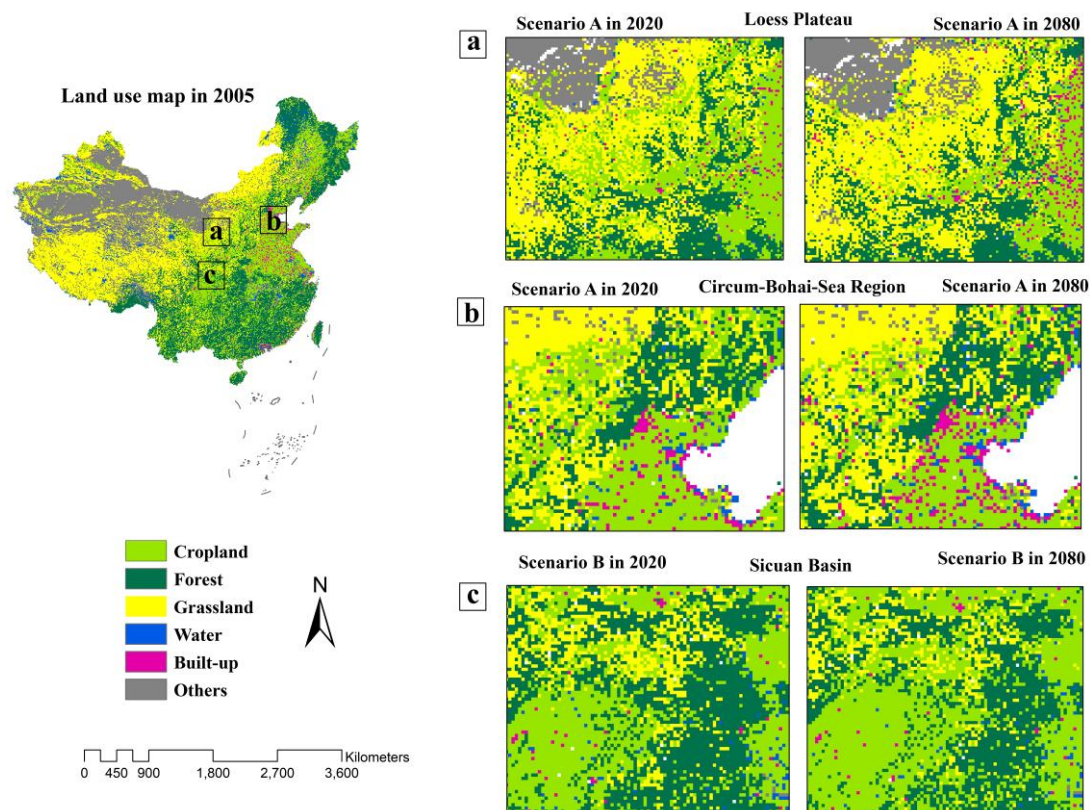


Figure 7. Hotspots of LULCC change in two scenarios. (a) Comparison between 2020 and 2080 under Scenario A in the Loess Plateau. (b) Comparison between 2020 and 2080 under Scenario A in the Circum-Bohai-Sea Region. (c) Comparison between 2020 and 2080 under Scenario B in the Sichuan Basin.

Figure 8 displays the different spatial distribution patterns predicted in both scenarios. Also, it shows how LULCC is affected by the different effects of the yield change that is expected to occur. Comparing Scenario A with Scenario B, we can see that the reduction of cropland will most likely be mainly distributed in the Loess Plateau farming-pastoral areas and Inner Mongolia, where the cropland will be converted into grassland. In the south and southwest mountains, where the reclamation of terraces on steep slopes easily leads to soil erosion and natural disasters, cropland will be converted into forests. Some croplands on the North China Plain and in the eastern coastal areas may restrain the expansion of cities and are more likely to be converted into built-up areas. At the same time, fertile soil is expected to contribute to the high yield of grain in the Northeast Plain, the Huang-Huai-Hai Plain, and the Sichuan Basin, all of which are places where cropland is expected to remain stable.

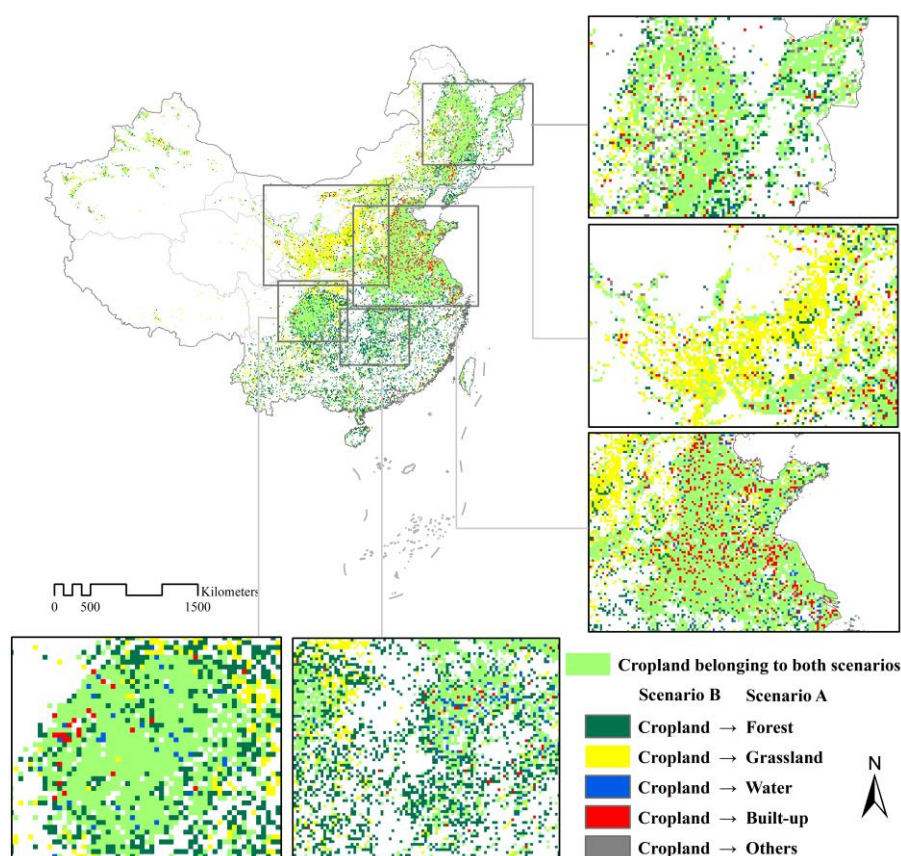


Figure 8. Comparison of land use types between two scenarios for the year 2080.

4. Discussion

Given the broad range of future uncertainties, LULC projection could be a useful tool that allows land managers to visualize alternative landscape futures, improve planning, and optimize management practices. Multiple processes lead to complex and interdependent dynamics under the condition of cross-scale and multi-factor interactions [59,60]. It is difficult to analyze and subsequently simulate complicated social phenomena and realities, such as technological development, implementation of agricultural policies, and the increasing demand for food. However, integrative modeling is designed to abstract and extract the real world as much as possible. When thinking of “strong” sustainability, rapid economic development at the expense of environmental quality is not to be considered as being sustainable [29]. Therefore, these measures, which are a part of human intervention, should be added to the ecological processes module in order to take into account the effects on soil organic matter and soil nitrogen. Before governments and stakeholders make land use decisions, local environmental conditions should first be assessed in order to identify stable equilibrium points between ecological efficiency and economic profit.

The results of this integrated model for China illustrate an exploration of future spatial dynamics of LULCC in different scenarios, and they agree with the results of Xu [8] and Liu [61]. In Scenario A, the growing efficiency of land use and the intensification of agricultural production leads to a reduction in demand for cropland, so more land can be returned to nature to increase ecological benefits. This is in line with the goals of the China Grain for Green Program [62]. Cropland in the southwestern mountains and southern low hill areas face land abandonment owing to steep slopes and poor nutrients [63,64]. The vulnerable ecological conditions here render it susceptible to damage due to soil erosion. Therefore, areas such as those listed above are presumed to be returned to grasslands or forests, which is consistent with the Sloping Land Conversion Program in China [63,64]. In Scenario B, yield stays constant, and as the population increases, the area of cropland significantly increases as

well. This cropland expansion is expected to cause massive deforestation and will consume many of the lands that have been set aside for conservation, so there is a consequential reduction in ecological benefits for the region. Compared with land use in different periods, all land use types in Scenario B have significantly fewer areas than those in Scenario A, excluding cropland. Extensive agricultural production requires more arable land, China may require twice or three times croplands to meet current food demands [65]. Some grasslands and forests are expected to be converted into cropland, especially the inter-mountains in the south of China, and the expansion of cropland may cause the severe degradation of natural environments.

The role of China is important for maintaining future global food security, not only by reducing its own hunger index, but also by increasing multilateral trade and technology exchanges. China is expected to be the world's second largest importer and exporter by 2020, and it will shift its status from net exporter to net importer in order to be self-sufficient in the future, bringing opportunities for agricultural development and cropland adjustment in many countries, especially developing countries [66]. However, importing food products is the equivalent of exporting ecological impacts [66]. In other words, cropland in China that is converted back into conservation land can essentially be perceived as the direct displacement of ecological lands by croplands in other countries [67]. Therefore, increasing yield through technology could not only ensure China's food security goals and continued economic prosperity, but could also contribute to achieving sustainable development goals on a global scale via trade flow. Being well-integrated among nations in matters of trade can also contribute to increasing land use efficiency via regional specialization and increased productivity. However, the homogenization of cultivation practices may lead to the simplification of ecosystem services; this phenomenon has been shown to indicate the declining resilience and growing instability of a land system [68,69]. Especially in arid and semi-arid regions, the dual pressure of economic development and ecological degradation may increase the vulnerability of land systems.

Technological advancement is one of the main mechanisms of boosting yield. There is a positive feedback cycle between increasing yield and returning farmland to forests/grassland [70]. In the Loess Plateau, the increase in yield has saved more cropland, reflecting the implementation of the Grain for Green Program in the past decade. Then, because of the implication of the program, the area of sloping farmland with thin harvests has been greatly reduced. More production technologies, such as agricultural mechanization, can be developed for high-yield cropland, thus maintaining high-yield and stable production. Scenario A is more promising for a sustainable land system; the ecological environment is maintained and improved while meeting human needs because of the positive feedback. From 1979 to 2016, the amount of N, P, and K fertilizer used in agricultural land in China increased by 179.8%, 271.4%, and 1915.5%, respectively (China Statistical Yearbook). Regrettably, too much fertilization can lead to soil degradation and water eutrophication in low-yield agricultural systems [71]. Farming accounts for approximately 70% of the water used worldwide, and some irrigation processes may lead to water pollution from excess nutrients, soil salinization, and other contamination [72,73]. Continuous investments are still required for advanced technologies to reduce pollutants and limit soil erosion. Furthermore, cropping intensity is needed for China to rely on to enhance the production and decrease the LRF by increasing the effective area of cropping [74].

The results of this simulation only represent a possible blueprint for future LULCC. However, it must be understood that this comes with great uncertainty regarding the environment, national policy, economic development, and other factors. On the one hand, integrated modeling assumes that the relationship between land use change and multiple driving factors is stable or shows little variation in the short term. On the other hand, model parameters, such as spatial policies and restrictions and the stability of land use conversions, are set using expert knowledge or observed behavior in the recent past and incorporate a certain degree of uncertainty. These scenario conditions are set to simulate possible trends of land use change in the future. In the future, we will improve the simulation in the following aspects. First, we will use medium- to high-resolution remote sensing data to quantify LULCC with greater precision [75]. Second, we will combine more ecological effects, such as soil moisture and net

primary production to assess local suitability. Third, the IMAGE model can be used to evaluate the mechanisms that how import or export of agricultural commodities influence on LULCC [76].

5. Conclusions

In this study, a global food model was used to represent the major impacts of socioeconomics on land-use demands; we addressed ecological effects and integrated the LULCC dynamics into this model.

The coupling model was applied in order to simulate future land use patterns for 2020, 2050, and 2080 in China under two scenarios with different yield rates. The results indicate numerous changes in land use. In Scenario A, the development of technology could save more land for ecological restoration and urbanization, and this potential result is in line with China's Grain for Green Program. In Scenario B, cropland is expected to be expanded in order to satisfy expected food demand, which may cause the degradation of ecological environments, especially in the areas with steep slopes. Regarding the sustainability of the human–environment system and given the limited opportunities and high costs associated with expanding agricultural land, Scenario A is the most promising scenario if environmental protection policy is strictly implemented with the simultaneous pursuit of economic development. This study could serve as a reference for planners of sustainable land use management.

Author Contributions: X.X. conceived, designed, and performed the experiments; H.J. and M.G. analyzed the data; Y.H. and Y.L. contributed materials and analysis tools; X.X. and H.J. wrote the paper. All authors reviewed the manuscript.

Funding: This research was funded by The National Key R&D Program of China, grant number 2017YFA0604902, the National Key Research and Development Program of China, grant number 2017ZX07301-001-03, The Foundation for Innovative Research Groups of the National Natural Science Foundation of China, grant number 41621061, Project Supported by State Key Laboratory of Earth Surface Processes and Resource Ecology.

Acknowledgments: We would like to thank Jianguo Wu (Arizona State University) and Lei Duan (Tsinghua University) for their comments and discussions on an earlier draft of this paper.

Conflicts of Interest: There is no conflict of interest. The founding sponsors had no role in the design of the study; in the collection, analyses, or interpretation of data; in the writing of the manuscript, and in the decision to publish the results.

References

1. Riebsame, W.E.; Meyer, W.B.; Turner, B.L. Modeling Land Use and Cover as Part of Global Environmental Change. *Clim. Chang.* **1994**, *28*, 45–64. [[CrossRef](#)]
2. Turner, B.L.; Meyer, W.B.; Skole, D.L. Global Land-Use/Land-Cover Change: Towards an Integrated Study. *Ambio. Stockholm.* **1994**, *23*, 91–95.
3. Xu, X.; Jiang, H.; Tian, X.; Guan, M.; Wang, L. Response of the Plant and Soil Features to Degradation Grades in Semi-arid Grassland of the Inner Mongolia, China. In *IOP Conference Series: Materials Science and Engineering*; IOP Publishing: Bristol, UK, 2019.
4. Lambin, E.F.; Geist, H.J.; Lepers, E. Dynamics of land-use and land-cover change in tropical regions. *Annu. Rev. Environ. Resour.* **2003**, *28*, 205–241. [[CrossRef](#)]
5. Liu, Z.; He, C.; Zhang, Q.; Huang, Q.; Yang, Y. Extracting the dynamics of urban expansion in China using DMSP-OLS nighttime light data from 1992 to 2008. *Landsc. Urban Plan.* **2012**, *106*, 62–72. [[CrossRef](#)]
6. Zheng, Q.; Yang, X.; Wang, K.; Huang, L.; Shahtahmassebi, A.R.; Gan, M.; Weston, M.V. Delimiting Urban Growth Boundary through Combining Land Suitability Evaluation and Cellular Automata. *Sustainability* **2017**, *9*, 2213. [[CrossRef](#)]
7. Zhao, Y.; Li, X. Spatial Correlation between Type of Mountain Area and Land Use Degree in Guizhou Province, China. *Sustainability* **2016**, *8*, 849. [[CrossRef](#)]
8. Xu, X.; Gao, Q.; Liu, Y.-H.; Wang, J.-A.; Zhang, Y. Coupling a land use model and an ecosystem model for a crop-pasture zone. *Ecol. Model.* **2009**, *220*, 2503–2511. [[CrossRef](#)]
9. Xu, X.; Gao, Q.; Peng, C.; Cui, X.; Liu, Y.; Jiang, L. Integrating global socio-economic influences into a regional land use change model for China. *Front. Earth Sci.* **2014**, *8*, 81–92. [[CrossRef](#)]

10. He, C.; Zhang, D.; Huang, Q.; Zhao, Y. Assessing the potential impacts of urban expansion on regional carbon storage by linking the LUSD-urban and InVEST models. *Environ. Model. Softw.* **2016**, *75*, 44–58. [[CrossRef](#)]
11. Gao, Q.; Yu, M.; Liu, Y.; Xu, H.; Xu, X. Modeling interplay between regional net ecosystem carbon balance and soil erosion for a crop-pasture region. *J. Geophys. Res. Space Phys.* **2007**, *112*, 527–531. [[CrossRef](#)]
12. Verburg, P.H.; Crossman, N.; Ellis, E.C.; Heinemann, A.; Hostert, P.; Mertz, O.; Nagendra, H.; Sikor, T.; Erb, K.-H.; Golubiewski, N.; et al. Land system science and sustainable development of the earth system: A global land project perspective. *Anthropocene* **2015**, *12*, 29–41. [[CrossRef](#)]
13. Liu, Z.; Yang, Y.; He, C.; Tu, M. Climate change will constrain the rapid urban expansion in drylands: A scenario analysis with the zoned Land Use Scenario Dynamics-urban model. *Sci. Total. Environ.* **2019**, *651*, 2772–2786. [[CrossRef](#)] [[PubMed](#)]
14. Verburg, P.H.; Soepboer, W.; Veldkamp, A.; Limpiada, R.; Espaldon, V.; Mastura, S.S.; Veldkamp, T. Modeling the Spatial Dynamics of Regional Land Use: The CLUE-S Model. *Environ. Manag.* **2002**, *30*, 391–405. [[CrossRef](#)] [[PubMed](#)]
15. Huang, Q.; He, C.; Liu, Z.; Shi, P. Modeling the impacts of drying trend scenarios on land systems in northern China using an integrated SD and CA model. *Sci China Earth Sci.* **2014**, *57*, 839–854. [[CrossRef](#)]
16. Brown, D.G.; Walker, R.; Manson, S.; Seto, K. Modeling Land Use and Land Cover Change. *Remote Sens. Digit. Image Process.* **2012**, *6*, 395–409.
17. Zhang, Y.; Wang, P.; Wang, T.; Cai, C.; Li, Z.; Teng, M. Scenarios Simulation of Spatio-Temporal Land Use Changes for Exploring Sustainable Management Strategies. *Sustainability* **2018**, *10*, 1013. [[CrossRef](#)]
18. Pei, B.; Pan, T. Land Use System Dynamic Modeling: Literature Review and Future Research Direction in China. *Prog. Geogr.* **2010**, *29*, 1585–1590.
19. Wang, R.; Derdouri, A.; Murayama, Y. Spatiotemporal Simulation of Future Land Use/Cover Change Scenarios in the Tokyo Metropolitan Area. *Sustainability* **2018**, *10*, 2056. [[CrossRef](#)]
20. Liu, X.; Liang, X.; Li, X.; Xu, X.; Ou, J.; Chen, Y.; Li, S.; Wang, S.; Pei, F. A future land use simulation model (FLUS) for simulating multiple land use scenarios by coupling human and natural effects. *Landsc. Urban Plan.* **2017**, *168*, 94–116. [[CrossRef](#)]
21. Parker, D.C.; Manson, S.M.; Janssen, M.A.; Hoffmann, M.J.; Deadman, P. Multi-Agent Systems for the Simulation of Land-Use and Land-Cover Change: A Review. *Ann. Assoc. Am. Geogr.* **2003**, *93*, 314–337. [[CrossRef](#)]
22. Verburg, P.; De Koning, G.; Kok, K.; Veldkamp, A.; Bouma, J.; Verburg, P.; Veldkamp, T. A spatial explicit allocation procedure for modelling the pattern of land use change based upon actual land use. *Ecol. Model.* **1999**, *116*, 45–61. [[CrossRef](#)]
23. Verburg, P.H.; Schot, P.P.; Dijst, M.J.; Veldkamp, A. Land use change modelling: Current practice and research priorities. *Geojournal* **2004**, *61*, 309–324. [[CrossRef](#)]
24. Han, H.; Yang, C.; Song, J. Scenario Simulation and the Prediction of Land Use and Land Cover Change in Beijing, China. *Sustainability* **2015**, *7*, 4260–4279. [[CrossRef](#)]
25. Losiri, C.; Nagai, M.; Ninsawat, S.; Shrestha, R.P. Modeling Urban Expansion in Bangkok Metropolitan Region Using Demographic–Economic Data through Cellular Automata-Markov Chain and Multi-Layer Perceptron-Markov Chain Models. *Sustainability* **2016**, *8*, 686. [[CrossRef](#)]
26. Deng, X.; Jiang, Q.; Zhan, J.; He, S.; Lin, Y. Simulation on the dynamics of forest area changes in Northeast China. *J. Geogr. Sci.* **2010**, *20*, 495–509. [[CrossRef](#)]
27. Trisurat, Y.; Shirakawa, H.; Johnston, J.M. Land-Use/Land-Cover Change from Socio-Economic Drivers and Their Impact on Biodiversity in Nan Province, Thailand. *Sustainability* **2019**, *11*, 649. [[CrossRef](#)]
28. Bakker, M.M.; Opdam, P.F.M.; Jongman, R.H.G.; Brink, A.V.D. Model explorations of ecological network performance under conditions of global change. *Landsc. Ecol.* **2015**, *30*, 763–770. [[CrossRef](#)]
29. Li, X.; Chen, G.; Liu, X.; Liang, X.; Wang, S.; Chen, Y.; Pei, F.; Xu, X. A New Global Land-Use and Land-Cover Change Product at a 1-km Resolution for 2010 to 2100 Based on Human–Environment Interactions. *Ann. Am. Assoc. Geogr.* **2017**, *107*, 1040–1059. [[CrossRef](#)]
30. Meyer, W.B.; Turner, B.L. Human population growth and global land-use/cover change. *Annu. Rev. Ecol. Syst.* **1992**, *1*, 39–61. [[CrossRef](#)]
31. Le, Q.B.; Park, S.J.; Vlek, P.L.G.; Cremers, A.B. Land-Use Dynamic Simulator (LUDAS): A multi-agent system model for simulating spatio-temporal dynamics of coupled human–landscape system. I. Structure and theoretical specification. *Ecol. Inform.* **2008**, *3*, 135–153. [[CrossRef](#)]

32. Qi, J.; Chen, J.; Wan, S.; Ai, L. Understanding the coupled natural and human systems in Dryland East Asia. *Environ. Res. Lett.* **2012**, *7*, 015202. [[CrossRef](#)]
33. Verburg, P.H.; Overmars, K.P. Combining top-down and bottom-up dynamics in land use modeling: Exploring the future of abandoned farmlands in Europe with the Dyna-CLUE model. *Landsc. Ecol.* **2009**, *24*, 1167–1181. [[CrossRef](#)]
34. Hirsch, B.J. Natural support systems and coping with major life changes. *Am. J. Community Psychol.* **1980**, *8*, 159–172. [[CrossRef](#)]
35. Stead, D. Relationships between Land Use, Socioeconomic Factors, and Travel Patterns in Britain. *Environ. Plan. B Plan. Des.* **2001**, *28*, 499–528. [[CrossRef](#)]
36. Heisey, P. *The Conditions of Agricultural Growth: The Economics of Agrarian Change under Population Pressure: Ester Boserup*; Earthscan Publications Ltd.: London, UK, 1993; 124p.
37. *World Population Projected to Reach 9.7 Billion by 2050*; United Nations Department of Economic and Social Affairs: New York, NY, USA, 2015.
38. Tilman, D.; Cassman, K.G.; Matson, P.A.; Naylor, R.; Polasky, S. Agricultural sustainability and intensive production practices. *Nature* **2002**, *418*, 671–677. [[CrossRef](#)]
39. Balmford, A.; Green, R.E.; Scharlemann, J.R.P.W. Sparing land for nature: Exploring the potential impact of changes in agricultural yield on the area needed for crop production. *Glob. Chang. Biol.* **2005**, *11*, 1594–1605. [[CrossRef](#)]
40. Lambin, E.F.; Meyfroidt, P. Global land use change, economic globalization, and the looming land scarcity. *Proc. Natl. Acad. Sci. USA* **2011**, *108*, 3465–3472. [[CrossRef](#)]
41. DeFries, R.S.; Rudel, T.; Uriarte, M.; Hansen, M. Deforestation driven by urban population growth and agricultural trade in the twenty-first century. *Nat. Geosci.* **2010**, *3*, 178–181. [[CrossRef](#)]
42. National Bureau of Statistics of the People’s Republic of China. *China Population and Employment Statistics Yearbook*; China Statistics Press: Beijing, China, 2018.
43. Kong, X.B. China must protect high-quality arable land. *Nature* **2014**, *506*, 7. [[CrossRef](#)]
44. Chen, W.; Carsjens, G.; Zhao, L.; Li, H. A Spatial Optimization Model for Sustainable Land Use at Regional Level in China: A Case Study for Poyang Lake Region. *Sustainability* **2015**, *7*, 35–55. [[CrossRef](#)]
45. National Bureau of Statistics of China. *China Statistical Yearbook 2014*; China Statistics Press: Beijing, China, 2014.
46. Dalgaard, P.; Emborg, J.; Kjølby, A.; Sørensen, N.; Ballin, N.Z. Histamine and biogenic amines: Formation and importance in seafood. In *Improving Seafood Products for the Consumer*; British Welding Research Association: Cambridge, UK, 2008; pp. 292–324.
47. Gibbs, H.K.; Ruesch, A.S.; Achard, F.; Clayton, M.K.; Holmgren, P.; Ramankutty, N.; Foley, J.A. Tropical forests were the primary sources of new agricultural land in the 1980s and 1990s. *Proc. Natl. Acad. Sci. USA* **2010**, *107*, 16732–16737. [[CrossRef](#)] [[PubMed](#)]
48. Uchida, E.; Rozelle, S.; Xu, J. Conservation Payments, Liquidity Constraints, and Off-Farm Labor: Impact of the Grain-for-Green Program on Rural Households in China. *Am. J. Agric. Econ.* **2009**, *91*, 70–86. [[CrossRef](#)]
49. Ewers, R.M.; Scharlemann, J.P.W.; Balmford, A.; Green, R.E. Do increases in agricultural yield spare land for nature? *Glob. Chang. Boil.* **2009**, *15*, 1716–1726. [[CrossRef](#)]
50. Tilman, D. The Ecological Consequences of Changes in Biodiversity: A Search for General Principles. *Ecol.* **1999**, *80*, 1455. [[CrossRef](#)]
51. Green, R.E.; Cornell, S.J.; Scharlemann, J.P.; Balmford, A. Farming and the fate of wild nature. *Science* **2005**, *307*, 550–555. [[CrossRef](#)] [[PubMed](#)]
52. Mooney, H.; Cropper, A.; Reid, W. Confronting the human dilemma. *Nature* **2005**, *434*, 561. [[CrossRef](#)] [[PubMed](#)]
53. Harris, J.M.; Kennedy, S. Carrying capacity in agriculture: Global and regional issues. *Ecol. Econ.* **1999**, *29*, 443–461. [[CrossRef](#)]
54. FAO. *Statistical Databases*; FAO: Rome, Italy, 2018.
55. Wu, J. Landscape sustainability science: Ecosystem services and human well-being in changing landscapes. *Landsc. Ecol.* **2013**, *28*, 999–1023. [[CrossRef](#)]
56. Jiang, L.; Cui, X.F.; Xu, X. A simple global food system model. *Agric. Econ-Blackwell* **2014**, *60*, 188–197. [[CrossRef](#)]

57. World Health Organization. Diet, Nutrition and the Prevention of Chronic Diseases. Available online: http://whqlibdoc.who.int/trs/WHO_TRS_916.pdf (accessed on 14 January 2014).
58. Brown, M.E.; Funk, C.C. Food Security Under Climate Change. *Sci.* **2008**, *319*, 580–581. [[CrossRef](#)] [[PubMed](#)]
59. Verburg, P.H.; Eickhout, B.; van Meijl, H. A multi-scale, multi-model approach for analyzing the future dynamics of European land use. *Ann. Reg. Sci.* **2008**, *42*, 57–77. [[CrossRef](#)]
60. Veldkamp, A.; Verburg, P.; Veldkamp, T.; Verburg, P. Modelling land use change and environmental impact. *J. Environ. Manag.* **2004**, *72*, 1–3. [[CrossRef](#)] [[PubMed](#)]
61. Liu, J.; Kuang, W.; Zhang, Z.; Xu, X.; Qin, Y.; Ning, J.; Zhou, W.; Zhang, S.; Li, R.; Yan, C.; et al. Spatiotemporal characteristics, patterns, and causes of land-use changes in China since the late 1980s. *J. Geogr. Sci.* **2014**, *24*, 195–210. [[CrossRef](#)]
62. Bryan, B.A.; Gao, L.; Ye, Y.; Sun, X.; Connor, J.D.; Crossman, N.D.; Stafford-Smith, M.; Wu, J.; He, C.; Yu, D.; et al. China's response to a national land-system sustainability emergency. *Nature* **2018**, *559*, 193–204. [[CrossRef](#)] [[PubMed](#)]
63. Bennett, M.T. China's sloping land conversion program: Institutional innovation or business as usual? *Ecol. Econ.* **2008**, *65*, 699–711. [[CrossRef](#)]
64. Liu, Y.; Fu, B.; Lü, Y.; Wang, Z.; Gao, G. Hydrological responses and soil erosion potential of abandoned cropland in the Loess Plateau, China. *Geomorphology* **2012**, *138*, 404–414. [[CrossRef](#)]
65. Grosjean, P.; Kontoleon, A. How Sustainable are Sustainable Development Programs? The Case of the Sloping Land Conversion Program in China. *World Dev.* **2009**, *37*, 268–285. [[CrossRef](#)]
66. Nath, R.; Luan, Y.; Yang, W.; Yang, C.; Chen, W.; Li, Q.; Cui, X. Changes in Arable Land Demand for Food in India and China: A Potential Threat to Food Security. *Sustainability* **2015**, *7*, 5371–5397. [[CrossRef](#)]
67. Mayer, A.L.; Kauppi, P.E.; Angelstam, P.K.; Zhang, Y.; Tikka, P.M. Ecology. Importing timber, exporting ecological impact. *Science* **2005**, *308*, 359–360. [[CrossRef](#)]
68. Hossain, M.S.; Eigenbrod, F.; Johnson, F.A.; Dearing, J.A. Unravelling the interrelationships between ecosystem services and human wellbeing in the Bangladesh delta. *Int. J. Sustain. Dev. World Ecol.* **2016**, *24*, 120–134. [[CrossRef](#)]
69. Rockström, J.; Steffen, W.; Noone, K.; Persson, Å.; Chapin, F.S., III; Lambin, E.F.; Lenton, T.M.; Scheffer, M.; Folke, C.; Schellnhuber, H.J.; et al. A safe operating space for humanity. *Nature* **2009**, *461*, 472–475. [[CrossRef](#)] [[PubMed](#)]
70. Feng, Z.H. Research on Response Relationship between Food Security and Ecological Construction the Loess Plateau. Master's Thesis, Xi'an University of Technology, Xi'an, China, June 2018.
71. Gomiero, T. Soil Degradation, Land Scarcity and Food Security: Reviewing a Complex Challenge. *Sustainability* **2016**, *8*, 281. [[CrossRef](#)]
72. Prosdoci, M.; Burguet, M.; Di Prima, S.; Sofia, G.; Terol, E.; Comino, J.R.; Cerdà, A.; Tarolli, P. Rainfall simulation and Structure-from-Motion photogrammetry for the analysis of soil water erosion in Mediterranean vineyards. *Sci. Total. Environ.* **2017**, *574*, 204–215. [[CrossRef](#)] [[PubMed](#)]
73. Lal, R. Restoring Soil Quality to Mitigate Soil Degradation. *Sustainability* **2015**, *7*, 5875–5895. [[CrossRef](#)]
74. Siebert, S.; Portmann, F.T.; Döll, P. Global Patterns of Cropland Use Intensity. *Remote Sens.* **2010**, *2*, 1625–1643. [[CrossRef](#)]
75. Liu, Z.; Ding, M.; He, C.; Li, J.; Wu, J. The impairment of environmental sustainability due to rapid urbanization in the dryland region of northern China. *Landsc. Urban Plan.* **2019**, *187*, 165–180. [[CrossRef](#)]
76. Bouwman, A.F.; Kram, T.; Klein Goldewijk, K. Integrated modelling of global environmental change. *Overv. Image* **2006**, *2*, 225–228.

